ISSN 0030-400X, Optics and Spectroscopy, 2015, Vol. 119, No. 2, pp. 280–285. © Pleiades Publishing, Ltd., 2015.
Original Russian Text © I.A. Budagovsky, A.S. Zolot'ko, D.L. Korshunov, M.P. Smayev, S.A. Shvetsov, M.I. Barnik, 2015, published in Optika i Spektroskopiya, 2015, Vol. 119, No. 2, pp. 295–301.

PHYSICAL OPTICS

Generation of Spiral Dislocation of Wave Front in Absorbing Nematic Liquid Crystal

I. A. Budagovsky[a], A. S. Zolot'ko[a], D. L. Korshunov[a, b], M. P. Smayev[a], S. A. Shvetsov[a, b], and M. I. Barnik[c]

[a] *Lebedev Physical Institute, Russian Academy of Sciences, Moscow, 119991 Russia*
[b] *Moscow Institute of Physics and Technology, Dolgoprudnyi, Moscow oblast, 141700 Russia*
[c] *Shubnikov Institute of Crystallography, Russian Academy of Sciences, Moscow, 119333 Russia*
e-mail: smayev@lebedev.ru

Received March 12, 2015

Abstract—It is demonstrated that an optical beam acquires a component with spiral dislocation of wave front (optical vortex) due to passage through a layer of homeotropically aligned nematic liquid crystal with light-absorbing admixture. The vortex is formed owing to the heating of liquid crystal and transition to isotropic phase in the irradiated region, which leads to the generation of axisymmetric field distribution of director at the interface of the isotropic channel and nematic liquid crystal.

DOI: 10.1134/S0030400X15080044

INTRODUCTION

Optical beams with helical dislocations of wave front [1, 2], the so called optical vortices (OVs), attract much attention in recent years [3, 4]. The spiral character of phase leads to a singularity at the beam axis, so that the intensity in the central region is zero and the transverse intensity distribution is ring-shaped with a central minimum. The interest in OV is related to multiple applications (e.g., optical tweezers [5–7], systems for optical data transmission and processing [8–10], visualization of astronomical objects [11, 12], etc.).

The methods for the OV generation are based on the application of spiral retardation plates and axicons [4, 13, 14], dynamic holograms [6, 15], cylindrical lenses [16], and propagation of a focused beam along the optical axis of crystal [17–19]. Note also that OVs can be generated with the aid of cells with nematic liquid crystals (NLCs) [20–27]. NLCs are substantially anisotropic media the optical properties of which can easily be controlled using variations in external fields, temperature, boundary conditions, etc. In systems that employ NLCs for OV generation, a defect of orientation of the director field (a unit vector that is determined by the dominant orientation of the molecules of liquid crystal and directed along the optical axis) is generated [20, 21]. The director distribution depends on the azimuthal angle, and the dependence is determined by topological charge q of defect. An OV with a charge $m = 2q$ is formed when a circularly polarized beam passes through a layer with such a defect. In this case, the OV represents a circularly polarized beam in which the rotation direction of optical field is opposite to the rotation direction of the field of the incident (reference) beam.

In addition to the topological charge [20], phase difference δ between ordinary and extraordinary waves at the thickness of the sample can be used to characterize q-plates [20]. The energy of the incident beam is totally transferred to the OV at $\delta = \pi$, so that the method strongly depends on the wavelength of the incident beam. Such a problem can be solved using thermal action [22] or effect of external field [23–25] on the NLC birefringence.

The axisymmetric defect of orientation of the director field in NLC can be generated with the aid of the rubbing of aligning substrates that leads to radially symmetric boundary conditions [20–23] or photoalignment of deposited polymer [23, 24]. The application of natural defects of orientation in the disordered NLC layer (defects of the schlieren texture) is also possible [25]. A nematic droplet in water that exhibits radially symmetric distribution of the director field can also be used as a liquid-crystalline object that forms an OV upon passage of circularly polarized radiation [26].

A method for the OV generation in a homeotropically oriented NLC cell (low-frequency anisotropy $\Delta\varepsilon < 0$) in the absence of a preliminary formed defect under the action of subthreshold electric field was proposed in [27]. A photoconducting layer was deposited on a substrate of the cell, and irradiation caused the generation of charges and amplification of the low-frequency field in the irradiated region. The consequent local threshold exceedance and axisymmetric

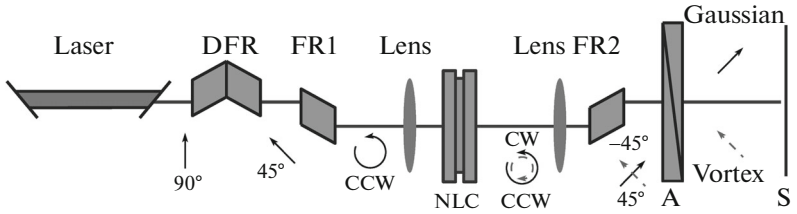

Fig. 1. Scheme of the experimental setup: DFR is double Fresnel rhomb, FR1 and FR2 are Fresnel rhombs, NLC is the cell with nematic liquid crystal, A is analyzer, and S is the screen. The arrows show the polarization of radiation. The linear polarization is rotated relative to the horizontal direction. The solid and dashed arrows correspond to the reference and vortex beams, respectively. The arrows in front of the screen show the direction of polarization of the analyzer that is needed for visualization of the corresponding component.

reorientation of the director led to the formation of defect needed for the OV generation.

In the aforementioned works, a necessary condition for the OV generation involves the spatial matching of the beam and defect (phase object) or application of strongly convergent beams or external fields.

In this work, we propose a method for OV generation with the aid of a circularly polarized beam passing through a dye-doped NLC that does not contain preliminary prepared defects and in the absence of external field. The axisymmetric field of director is formed due to the local phase transition NLC–isotropic liquid owing to heating.

SAMPLES AND EXPERIMENTAL SETUP

We use a ZhKM-1277 (NIOPIK) matrix with a nematic phase at temperatures ranging from –20 to +60°C. The refractive indices of the extraordinary and ordinary waves at a wavelength of $\lambda = 589$ nm are 1.71 and 1.52, respectively. The NLC is doped with methyl red dye (MR):

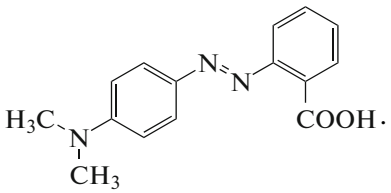

The liquid-crystalline mixture is placed in a plane-parallel cell that consists of two glass substrates the distance between which is 100 μm. The admixture concentration is 0.3 wt %, and the absorption spectrum of the mixture is peaked at $\lambda = 510$ nm. The absorption coefficient of the ordinary wave at a wavelength of $\lambda = 532$ nm is $\alpha_o = 160$ cm^{-1}. The homeotropic orientation of the NLC (director **n** is orthogonal to the substrates) is generated using an aligning layer of chromium stearyl chloride that is deposited with the aid of centrifuging and thermally processed.

Figure 1 shows the scheme of the experimental setup. We use linearly polarized radiation of a LASOS Lasertechnik GL-V6 solid-state laser with a radiation wavelength of $\lambda = 532$ nm. The radiation passes through a system of polarization elements (double Fresnel rhomb (DFR) and Fresnel rhomb (FR1)) and is focused by a lens with $f = 6$ cm. The beam waist is $w_0 \approx 30$ μm on the NLC cell. The DFR rotation relative to the beam axis makes it possible to form linear or circular polarization. The radiation is incident on the NLC along the normal, and the wave vector is parallel to unperturbed director $\mathbf{n}_0$. The beam transmitted by the NLC cell passes through the second Fresnel rhomb (that transforms the circular polarization into linear one) and a film polarizer. We can separately analyze the reference and vortex beams with opposite circular polarizations, since the second Fresnel rhomb (FR2) transforms the circular polarizations into mutually orthogonal linear polarizations. The transverse intensity distribution of the transmitted beam is observed on a screen.

EXPERIMENTAL RESULTS

Formation of Isotropic Channel

Figure 2 presents the photographs of the transverse intensity distribution of the optical beam having passed through the liquid-crystalline cell. The incident beam is circularly polarized. The experiments are performed in the absence of FR2 and analyzer. It is seen that a gradual increase in the power of the beam that is incident on the NLC leads to the formation of an aberration pattern in the far-field zone and, then, disappearance of such a pattern.

At a power of $P = 0.2$–5 mW (Figs. 2a–2c), we observe a system of aberration rings the divergence and characteristic time for which correspond to the thermal nonlinearity (i.e., bell-shaped variation in the refractive index owing to local heating of the sample). A further increase in the power results in the suppression of the aberration pattern, so that its contrast and divergence decrease (Figs. 2d–2f). Such a transformation of the intensity distribution is related to the formation of a channel of isotropic liquid along the beam axis (Fig. 3a) due to heating [28, 29]. The director of NLC tends to normal orientation relative to the boundary of such a cylindrical channel, so that an

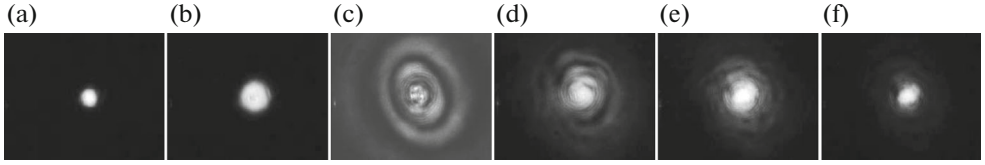

Fig. 2. Transverse intensity distribution of the optical beam having passed through ZhKM-1277 + 0.3% MR for optical powers of P = (a) 0.2, (b) 2, (c) 5, (d) 8, (e) 14, and (f) 17 mW. Distributions (a)–(c) correspond to an increase in the thermal nonlinearity and an increase in the size of the aberration pattern (formation of the nonlinear lens), and distributions (e), (f) correspond to the transformation of the nonlinear lens into an isotropic channel and, hence, a decrease in the beam divergence.

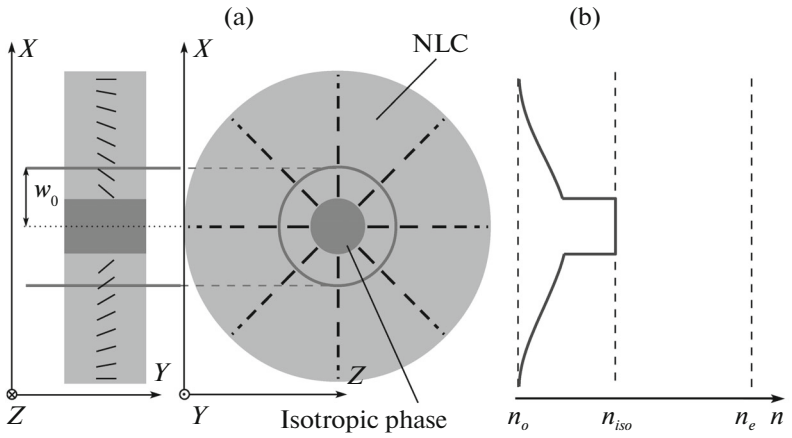

Fig. 3. (a) Scheme of the formation of the isotropic channel in the NLC in the irradiated region (the segments show the directions of the director (optical axis)) and (b) profile of the refractive index (n_o is the refractive index of ordinary wave, n_e is the refractive index of extraordinary wave, and n_{iso} is the refractive index of isotropic phase).

axisymmetric field of director is formed inside the irradiated region, which is needed for OV generation. In addition, the distribution of the refractive index ceases to be bell-shaped in accordance with the intensity profile of the beam (as would be in the presence of thermal nonlinearity) and a region that corresponds to the refractive index of isotropic phase is formed (Fig. 3b).

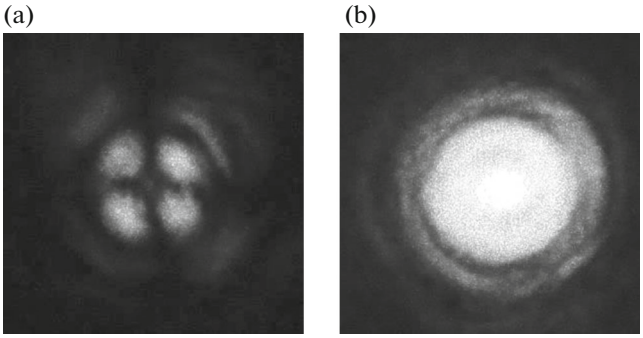

Fig. 4. Intensity distribution of the optical beam (λ = 532 nm and P = 18 mW) in the far-field zone behind the analyzer the axis of which is (a) perpendicular and (b) parallel to the polarization of the incident beam.

Note the absence of effects related to the light-induced reorientation of director in such a configuration. This result is due to the fact that the MR dye induces negative orientational nonlinearity in ZhKM-1277 and the optical torque provides the stabilization of the original homeotropic orientation of the NLC. When the isotropic channel is formed, optical orientational effects are relatively weak in comparison with the thermal effects.

When the NLC is irradiated by a linearly polarized beam at a power that is sufficient for the formation of the isotropic channel (the experimental results are presented for a power of P = 18 mW), we observe a dark cross in the crossed polarizers, which is typical of a point defect [29] (Fig. 4a). When the analyzer is parallel to the polarization plane of the incident beam, we observe diffraction equidistant rings (Fig. 4b). The distance between the rings can be used to determine channel diameter D that provides the diffraction of radiation: $D = \lambda/\Delta\Theta$ (λ is the radiation wavelength, and $\Delta\Theta$ is the angular distance between the neighboring rings). The channel dimension was estimated as D = 30 μm.

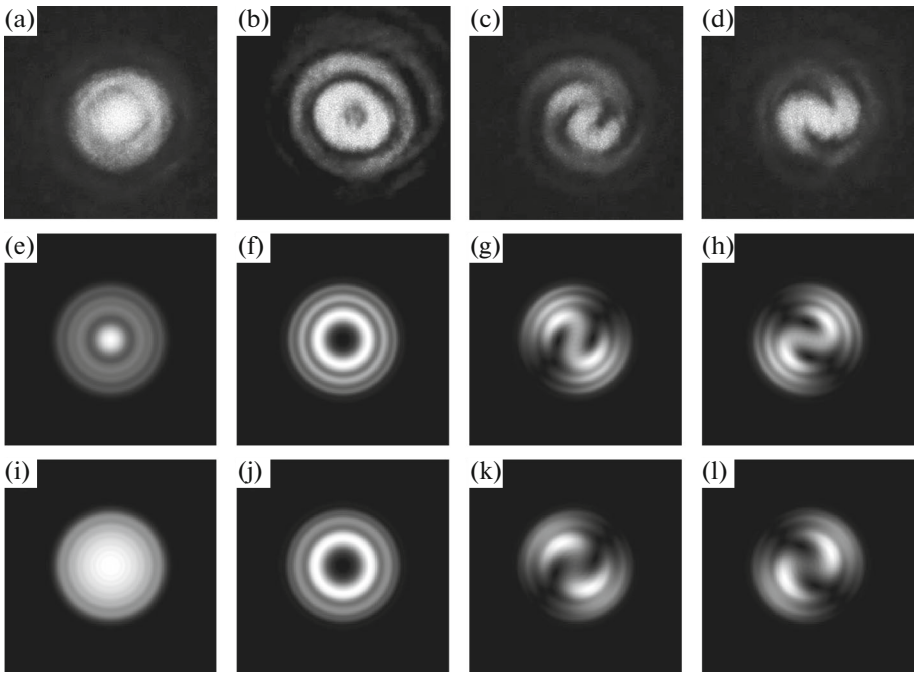

Fig. 5. (a)–(d) Experimental and (e)–(l) theoretical intensity distributions of the optical beam ($\lambda = 532$ nm and $P = 18$ mW) having passed through the liquid-crystalline layer. The distributions are obtained in the far-field zone behind the analyzer for (a), (e), (i) reference component (in the absence of vortex); (b), (f), (g) vortex component; and the interference of the reference and vortex components at analyzer positions of (c), (g), (k) 0° and (d), (h), (l) 90°. The angular size of the frames is 0.1 rad. The patterns in panels (e)–(h) are calculated for the Gaussian distribution of the refractive index with the central step, and patterns in panels (i)–(l) are calculated for the Gaussian distribution of the refractive index.

Generation of Optical Vortex on Isotropic Channel in NLC

To generate the OV, we use the same beam that forms the needed deformation of the director. The effect of the axisymmetric director field (that emerges due to formation of an isotropic channel in an NLC) on the phase of the transmitted beam is similar to the effect of a point defect of orientation with a charge of $q = 1$. The passage of a circularly polarized beam through such a structure leads to the generation of OV with a charge of $m = \pm 2$. Here, the sign depends on the polarization direction (clockwise or counterclockwise) of the incident beam.

The transformation of the incident beam into a vortex beam is determined by phase shift δ and is only partial. This results in two components of the optical field upon the passage of the NLC. The wave front of the first component is free of singularities. The intensity distribution corresponds to the diffraction by the defect of the incident Gaussian beam (Fig. 5a). The second component exhibits the ring-shaped intensity distribution (Fig. 5b) and the opposite (with respect to the incident beam) direction of the circular polarization. The FR2 and analyzer that are placed behind the NLC allow separate observations of the components: when the analyzer is rotated relative to the horizontal direction by an angle of +45° (–45°), we observe the vortex (reference) component.

To visualize the spiral-shaped pattern, the summation of the OV and the Gaussian beam with the spherical wave front is usually used (see, for example, [20]). In the present study, OV interferes with the reference component that acquires the needed curvature of the wave front due to passage through the deformed region of NLC. Analyzer angular positions of 0° (Fig. 5c) or 90° (Fig. 5d) make it possible to observe the interference of the vortex and reference beams. The spiral-shaped interference patterns (Figs. 5c and 5d) prove the presence of a beam with a vortex structure of the wave front It should be noted, that the first observations of a spiral in the transverse distribution of the radiation intensity under local thermal phase transition in an NLC were reported in [28], but the effects were not comprehensively interpreted.

The OV power in the experiments is $P \approx 1$ mW. The power may substantially be increased due to a decrease in the dye concentration. In this case, the vortex power can be sufficient for problems of optical manipulation, since the corresponding forces that provide the optical trapping of micron-size dielectric particles will exceed 1 pN [30].

CALCULATION OF INTENSITY DISTRIBUTION FOR VORTEX BEAM

We consider the transformation of the optical beam that propagates through the NLC with the light-

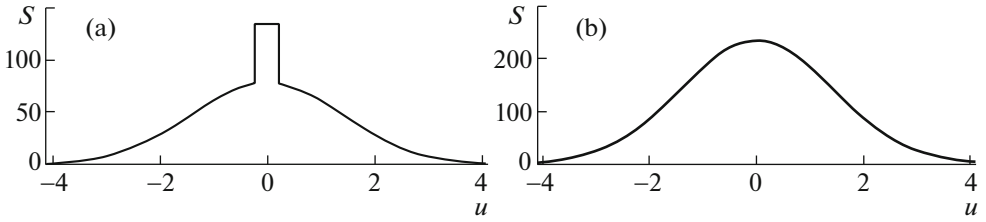

Fig. 6. Plots of the phase shift distributions that are employed in the calculations of the diffraction pattern: (a) Gaussian distribution with the central step and (b) Gaussian distribution.

induced isotropic channel. A beam focused on the NLC has initially the plane wave front and the Gaussian intensity distribution. The field of the incident beam is represented as

$$E_g(u) = A_0 e^{-u^2}, \tag{1}$$

where A_0 is the amplitude of the beam and u is the transverse coordinate in the plane of crystal that is normalized by beam waist w_0.

The absorption of radiation leads to NLC heating, so that an isotropic channel is formed at the central part of the irradiated region at a certain power. The NLC director is rotated by a certain angle at the boundary of the channel. The deformation of the director decreases with an increase in the distance from the interface. For simplicity, we assume that such a decrease leads to phase shift for the transmitted light in accordance with the Gaussian law

$$S_g(u) = kL\delta n e^{-bu^2}, \tag{2}$$

where is the parameter characterizing the change of refractive index averaged over NLC thickness; L is the thickness of the liquid-crystalline layer; $k = 2\pi/\lambda$ is the wave vector; and b is the dimensionless parameter that characterizes the size of the region of the director deformation. The effect of isotropic channel with width h is described using a step of a constant phase shift at the central region:

$$S_{iso} = kL\delta n_{iso}, \tag{3}$$

where δn_{iso} is the refractive index change due to nematic–isotropic phase transition.

Thus, the resulting phase shift is $S(u) = S_g(u)$ at $u \geq h$ and $S(u) = S_{iso}$ at $u < h$ (Fig. 6a).

To determine the transformation of the optical beam due to the effect of NLC, we employ the Jones matrices. In the basis of circular polarizations, the matrix that characterizes the passage through the homeotropically oriented NLC is written as

$$W = e^{i\frac{S_e(u)+S_o}{2}}\left\{\cos\frac{S(u)}{2}\begin{pmatrix}1 & 0\\ 0 & 1\end{pmatrix} + i\sin\frac{S(u)}{2}\begin{pmatrix}0 & e^{-2i\varphi}\\ e^{2i\varphi} & 0\end{pmatrix}\right\}, \tag{4}$$

where u and φ are the polar coordinates in the crystal plane and S_o and $S_e(u)$ are the phase shifts of the ordinary and extraordinary waves, respectively ($S(u) = S_e(u) - S_o$). When a circularly polarized wave $A_0\mathbf{e}_\pm$ (plus and minus correspond to the left and right circular polarizations, respectively) is incident on the cell, the field of the transmitted wave is given by

$$\mathbf{E} = WE_G\mathbf{e}_\pm = A_0 e^{-u^2} e^{iS_o + \frac{iS(u)}{2}}\left\{\cos\frac{S(u)}{2}\mathbf{e}_\pm + i\sin\frac{S(u)}{2}e^{\pm 2i\varphi}\mathbf{e}_\mp\right\}. \tag{5}$$

It is seen that the output beam is divided into two components. The polarization and intensity distribution of the first component correspond to the incident wave. The second component contains phase factor $e^{\pm 2i\varphi}$ and corresponds to the OV. It exhibits a spiral phase of the wave front, which leads to the minimum intensity at the central part of the beam, and circular polarization that is opposite to the polarization of the incident wave.

To calculate the amplitude of the optical beam having passed through the NLC, we use the Kirchhoff diffraction integral

$$\mathbf{E}_{\text{dif}}(R,\psi) = \frac{kw_0^2}{2\pi iz} e^{-\frac{ikR^2}{2z}} \int_0^\infty \int_0^{2\pi} \mathbf{E}(u,\varphi) \times e^{-\frac{iku^2w_0^2}{2z} - ik\frac{R}{z}\cos(\psi-\varphi)} u\,du\,d\varphi, \tag{6}$$

where R and ψ are the polar coordinates in the image plane and z is the distance from the crystal to the image plane. With allowance for the axial symmetry of the problem, we have $\mathbf{E}(u,\varphi) = \mathbf{E}(u)$. Substituting expression (5) in formula (6), we derive the expression

for the field of the optical wave having passed through the liquid-crystalline layer with the isotropic channel:

$$\mathbf{E}_{\text{dif}} = \frac{A_0 k w_0^2}{iz} e^{\frac{ikR^2}{2z}} \int_0^\infty u du e^{-u^2} e^{iS_0 + \frac{iS(u)}{2}} \times \left\{ \mathbf{e}_\pm \cos\frac{S(u)}{2} J_0(\tau u) - i\mathbf{e}_\mp e^{\pm 2i\psi} \sin\frac{S(u)}{2} J_2(\tau u) \right\}, \quad (7)$$

where $\tau = kw_0 R/z$ and J_0 and J_2 are the zero- and second-order Bessel functions, respectively. The intensity distributions of the diffraction patterns $I_{\text{dif}} = |\mathbf{E}_{\text{dif}}|^2$ that are calculated for several positions of the analyzer (Figs. 5e–5h) are in good agreement with the experimental results (Figs. 5a–5d).

The calculations with the Gaussian (rather than stepwise) profile of the phase shift (Fig. 6b) yield intensity distributions (Figs. 5i–5l) that are also in good agreement with the experimental data. Such a model corresponds to the significant intensity decay upon propagation of the optical beam when an isotropic droplet is formed instead of a cylindrical isotropic channel.

CONCLUSIONS

A method for generation of an optical vortex based on the passage of a circularly polarized beam through an NLC absorbing layer in the absence of preliminary formed defects and external fields is proposed. The vortex is generated due to formation of the axisymmetric director field related to the local heating of NLC and the development of isotropic channel. The results of calculations of the vortex generation are in good agreement with the experimental data.

ACKNOWLEDGMENTS

We are grateful to V.N. Ochkin for helpful discussions.

This work was supported by the Russian Science Foundation, project no. 14-12-00784.

REFERENCES

1. J. F. Nye and M. V. Berry, Proc. R. Soc. London, Ser. A **336**, 165 (1974).
2. V. Yu. Bazhenov, M. V. Vasnetsov, and M. S. Soskin, Pis'ma Zh. Eksp. Teor. Fiz. **52**, 1037 (1990).
3. A. S. Desyatnikov, Prog. Opt. **47**, 291 (2005).
4. V. V. Kotlyar and A. A. Kovalev, *Vortex Laser Beams* (Novaya Tekhnika, Samara, 2012) [in Russian].
5. N. B. Simpson, K. Dholakia, L. Allen, and M. J. Padgett, Opt. Lett. **22**, 52 (1997).
6. K. T. Gahagan and G. A. Swartzlander, Jr., J. Opt. Soc. Am. B **16**, 533 (1999).
7. M. Dienerowitz, M. Mazilu, P. J. Reece, T. F. Krauss, and K. Dholakia, Opt. Express **16**, 4991 (2008).
8. G. Molina-Terriza, J. P. Torres, and L. Torner, Nature Phys. **3**, 305 (2007).
9. M. S. Kirilenko and S. N. Khonina, Izvestiya Samarskogo Nauchnogo Tsentra RAN **14**, 292 (2012).
10. E. Nagali, F. Sciarrino, F. De Martini, L. Marrucci, B. Piccirillo, E. Karimi, and E. Santamato, Phys. Rev. Lett. **103**, 013601 (2009).
11. G. Foo, D. M. Palacios, and G. A. Swartzlander, Jr., Opt. Lett. **30**, 3308 (2005).
12. D. Mawet, E. Serabyn, K. Liewer, C. Hanot, S. McEldowney, D. Shemo, and N. O'Brien, Opt. Express **17**, 1902 (2009).
13. M. W. Beijersbergen, R. P. C. Coerwinkel, M. Kristensen, and J. P. Woerdman, Opt. Commun. **112**, 321 (1994).
14. *Methods for Computer Design of Diffractive Optical Elements*, Ed. by V. A. Soifer (Wiley, New York, 2002).
15. Y. J. Liu, X. W. Sun, Q. Wang, and D. Luo, Opt. Express **15**, 16645 (2007).
16. L. Allen, M. W. Beijersbergen, R. J. C. Spreeuw, and J. P. Woerdman, Phys. Rev. A **45**, 8185 (1992).
17. A. V. Volyar and T. A. Fadeeva, Opt. Spectrosc. **94** (2), 235 (2003).
18. A. Ciattoni, G. Cincotti, and C. Palma, J. Opt. Soc. Am. A **20**, 163 (2003).
19. E. Brasselet, Opt. Lett. **34**, 3229 (2009).
20. L. Marrucci, C. Manzo, and D. Paparo, Phys. Rev. Lett. **96**, 163905 (2006).
21. L. Marrucci, Mol. Cryst. Liq. Cryst. **488**, 148 (2008).
22. E. Karimi, B. Piccirillo, E. Nagali, L. Marrucci, and E. Santamato, Appl. Phys. Lett. **94**, 231124 (2009).
23. B. Piccirillo, V. D'Ambrosio, S. Slussarenko, L. Marrucci, and E. Santamato, Appl. Phys. Lett. **97**, 241104 (2010).
24. S. Slussarenko, A. Murauski, V. Chigrinov, L. Marrucci, and E. Santamato, Opt. Express **19**, 4085 (2011).
25. C. Loussert, U. Delabre, and E. Brasselet, Phys. Rev. Lett. **111**, 037802 (2013).
26. E. Brasselet, N. Murazawa, H. Misawa, and S. Juodkazis, Phys. Rev. Lett. **103**, 103903 (2009).
27. R. Barboza, U. Bortolozzo, G. Assanto, E. Vidal-Henriquez, M. G. Clerc, and S. Residori, Phys. Rev. Lett. **109**, 143901 (2012).
28. M. I. Barnik, A. S. Zolot'ko, and V. F. Kitaeva, Zh. Eksp. Teor. Fiz. **111**, 2059 (1997).
29. V. F. Kitaeva, N. N. Sobolev, N. N. Zolot'ko, N. Kroo, and L. Csillag, Mol. Cryst. Liq. Cryst. **91**, 137 (1983).
30. K. C. Neuman and S. M. Block, Rev. Sci. Instrum. **75**, 2787 (2004).